

***Radiometric Calibration of MSG SEVIRI Level 1.5  
Image Data in Equivalent Spectral Blackbody  
Radiance***

Doc.No. : EUM/OPS-MSG/TEN/03/0064  
Issue : v1  
Date : 17 January 2007

EUMETSAT  
Am Kavalleriesand 31, D-64295 Darmstadt, Germany  
Tel: +49 6151 807-7  
Fax: +49 6151 807 555 Telex: 419 320 metsat d  
<http://www.eumetsat.de>



## Table of Contents

<b>1</b>	<b>Purpose and Scope .....</b>	<b>5</b>
<b>2</b>	<b>Introduction .....</b>	<b>6</b>
2.1	The Spinning Enhanced Visible and Infrared Imager (SEVIRI) .....	6
2.2	Calibration.....	6
2.3	Overview.....	6
2.3.1	Solar Channel Calibration.....	6
2.3.2	Thermal Infrared Channel Calibration .....	7
<b>3</b>	<b>Calibration of Level 1.5 Image data and Population of Level 1.5 Headers .....</b>	<b>8</b>
3.1	Linearisation and Equalisation.....	8
3.2	Ground Characterisation, Vicarious Calibration and Blackbody Calibration .....	8
3.2.1	Ground Characterisation and Baseline Calibration .....	8
3.2.2	Blackbody Calibration .....	9
3.2.3	Vicarious Calibration.....	10
3.3	Current Operational Baseline .....	10
3.3.1	Thermal Channels .....	10
3.3.2	Solar Channels .....	11
3.3.3	Summary of Level 1.5 Data Production.....	11
<b>4</b>	<b>Details on Blackbody Calibration.....</b>	<b>13</b>
4.1	The SEVIRI Telescope .....	13
4.2	Black Body Calibration .....	14
4.3	Blackbody Models .....	15
4.3.1	Model 1 (EUMETSAT Scheme).....	15
4.3.2	Model 2 ("Portsmouth Scheme", "MMS-P Scheme") .....	15
4.3.3	Model 3 ("Toulouse Scheme", "MMS-F Scheme") .....	16
4.4	Application of Blackbody Calibrations in the Thermal channels.....	16
<b>5</b>	<b>Instrument Gain Changes and reduced Gain for Performance Assessment .....</b>	<b>17</b>
5.1	Degradation and Decontamination .....	17
5.2	Eclipse Season .....	19
<b>6</b>	<b>Reference Documents.....</b>	<b>20</b>
<b>Appendix A</b>	<b>Implementation of the Blackbody Models (from Volume Q of the IMPF DDD) .</b>	<b>21</b>
A.1	Method 1 (EUMETSAT Scheme) .....	23
A.2	Method 2 ("Portsmouth Scheme", "MMS-P Scheme") .....	24
A.3	Method 3 ("Toulouse Scheme", "MMS-F Scheme") .....	25
A.4	Derivation of Calibration Constant $K_{cal}$ .....	26

**Table of Contents**

Figure 1 – Schematic of the Scaling of Level 1.5 Counts .....	12
Figure 2 – Measurements and Direct Offset Correction .....	14
Figure 3 – Calibration Results for the IR 10.8 Channel outside an Eclipse Season (left) and during an Eclipse Season (right) .....	18
Figure 4 – Calibration Results for the IR 10.8 channel during 2003 .....	19

## **1 PURPOSE AND SCOPE**

It was found that there is no accurate description of the calibration of the SEVIRI Level 1.5 image data available. This document describes the full radiometric processing chain and its performance. Currently (End of 2006), the thermal infrared channels are calibrated in terms of **equivalent spectral blackbody radiance**, as described in this document. However, discrepancies in the published information have been identified by the Level 1.5 Image Product Oversight Panel (RD 1): The MSG Image Processing Facility generates Level 1.5 images in terms of **spectral blackbody radiance**. In contrast, the MSG Meteorological Product Extraction Facility, for historical reasons, works in terms of **effective blackbody radiance**. Information previously provided to the User community via the EUMETSAT web site describes the process used by the MPEF to convert MSG radiances to temperatures.

After careful consideration, EUMETSAT has concluded that, from the User perspective, the best way to resolve the inconsistency is to modify the MSG Image Processing Facility to generate Level 1.5 Image Products in terms of effective blackbody radiance rather than spectral blackbody radiance. An important argument for this is that it will bring the EUMETSAT approach in line with calibration scheme in use by other satellite operators. After the expected change to the processing, this document will be changed and re-issued.

## 2 INTRODUCTION

### 2.1 The Spinning Enhanced Visible and Infrared Imager (SEVIRI)

The overall SEVIRI layout is based on a compact three-mirror telescope and scan assembly. The 42 detectors of the twelve channels are accommodated in the telescope's focal plane in two areas, one at 20°C for solar channels (centred at wavelengths around 0.6, 0.8, 1.6µm and about 0.75µm for High Resolution Visible (HRV) channel). The thermal infrared detectors (centred at wavelengths around 3.9, 6.2, 7.3, 8.7, 9.7, 10.48, 12.0 and 13.4µm) are passively cooled down (to 85 K or 95K) to optimise their performance. The compact design allows the insertion of a small black body for full-pupil calibration. The response by every detector to the target's radiation is converted into an electronic signal by means of pre-amplifiers and a main detection unit including the ADC. The amplification can be adjusted to the needs at various stages of the signal processing. The full image processing from raw counts to Level 1.5 images is performed by the Image Processing Facility (IMPF).

### 2.2 Calibration

The End User Requirements specify that the "representation of the Level 1.5 images pixels be 10 bits ... as linearised function of radiance" (RD 2). This implies the following objectives for the radiometric calibration of the Level 1.5 images:

- to assure a linear relation between radiance and counts
- to assure an equalised response among detectors
- to apply the derived or received calibration information to the image data, therefore supplying a stable radiance-to-count relation for the Level 1.5 data.

The first two points refer to a pure relative calibration where the absolute relationship between counts and radiance is not considered, but rather that the detector output is linear and homogeneous over the whole image. The third point refers to the absolute calibration.

In the following, an overview presentation is made of how the various information sources are used to calibrate an image and to populate a Level 1.5 header. Following this, a more detailed explanation is supplied on the acquisition and processing of blackbody data. Thirdly, the processing performed is described in some detail. Information is repeated at various places. It is clear that this is redundant to some degree, however, it should facilitate the understanding of the relevant section in the full context.

### 2.3 Overview

#### 2.3.1 Solar Channel Calibration

As no on-board calibration device is available for the solar channels of MSG/SEVIRI, their calibration has to rely on a vicarious method. This method relies on radiative transfer modelling over bright desert and clear ocean sites. The choice of this method has been driven by the need to fulfil the accuracy and precision requirements of the MSG operational ground segment during the entire duration of the mission, i.e., more than 12 years. Radiative transfer simulations are performed with the 6S code, (RD 3), using a data set of surface and atmospheric properties. This data set is used to simulate SEVIRI observations accounting for the exact viewing and illumination conditions as well as the spectral characteristics of the

instrument. The duration of the MSG mission prohibits the continuous characterization of a limited number of targets with ground observations. The proposed strategy relies therefore on the definition of a large number of stable targets for which surface properties are estimated once and for all. The accuracy and precision of these calculated radiances are estimated comparing simulations with calibrated observations acquired by space borne instruments. An operational algorithm, named SEVIRI Solar Channel Calibration (SSCC), has been developed to ensure a routine calibration of the solar channels. First results show that SEVIRI solar channels can be calibrated with an estimated accuracy ranging from 4 to 6%, at the 95% confidence level, according to the band. (See RD 4).

### 2.3.2 Thermal Infrared Channel Calibration

In the current MSG calibration scheme, the SEVIRI thermal channels can be seen as a radiance thermometer. The calibrated radiance is provided as a spectral blackbody radiance equivalent in units of  $\text{mWm}^{-2}\text{sr}^{-1}(\text{cm}^{-1})^{-1}$ . The brightness temperature should therefore be calculated by just inverting the Planck function at the wavelength of the channel:

$$\frac{10^4}{\lambda_0} = \nu, \quad T_{BB} = \frac{c_2 \nu}{\ln \left[ 1 + \nu^3 \frac{c_1}{L} \right]}$$

with  $\lambda_0$  the central wavelength of the channel in  $\mu\text{m}$ .  $10^4/\lambda_0$  converts from wavelength in  $\mu\text{m}$  into wavenumber,  $\nu$ , in  $\text{cm}^{-1}$  ( $C_1=1.19104 \cdot 10^{-5} \text{ mW}(\text{cm}^{-1})^{-4} \text{ m}^{-2} \text{ sr}^{-1}$ ,  $C_2=1.43877 \text{ K cm}$ ).

### 3 CALIBRATION OF LEVEL 1.5 IMAGE DATA AND POPULATION OF LEVEL 1.5 HEADERS

#### 3.1 Linearisation and Equalisation

As pointed out in the introduction, linearisation is a high level requirement on the image processing. Not all SEVIRI detector response functions are linear in terms of absorbed energy ( $\int \tau(\lambda)Ld\lambda$ ,  $\tau$  spectral response) over the full range of radiance and may even change according to operating parameters, e.g. temperatures. Moreover, the finite bandwidth of the channel creates a non-linearity when comparing instrument response to spectral (blackbody) radiance.

The **non-linear behaviour** as well as the temperature dependence are already characterised on-ground and can be used by simply reversing the count-radiance relation, for the detector linearisation.

A perfect correction would also imply to correct for the differences in response between detectors within a channel (**equalisation**). However, the non-linear response curves are only known with a limited accuracy and may change over time for each individual detector. An effective equalisation of detectors has therefore to be based on detector output measurements. As all detectors see the “same” image in a statistical sense, the histograms from the data itself can be used to obtain this equalisation. One of the detectors, the central detector of the channel, is chosen as a reference. Then a mapping between outputs of each detector of the same spectral channel to that of the reference is sought that leads to an equal histogram distribution.

#### 3.2 Ground Characterisation, Vicarious Calibration and Blackbody Calibration

To ensure the required stability of the count-to-radiance relationship absolute calibration information is required. This information comes to the IMPF from three sources:

- ground characterisation,
- a feedback from MPEF (Meteorological Product Extraction Facility) that carries corrections of the currently applied calibration constants (vicarious calibration), and
- from the blackbody/deep space calibration that allows for the determination of the raw count-radiance relationship on board in the thermal infrared (IR) channels.

Please note, that for the solar channels no on-board calibration source is available and hence the calibration is either based on vicarious calibration or on ground characterisation.

##### 3.2.1 Ground Characterisation and Baseline Calibration

Ground characterisations are based on measurements made on the SEVIRI instrument on ground during testing. Among other things, they describe the response of the instrument (in **counts**) as a quadratic polynomial of incoming **spectral blackbody radiance**. This includes both, the effect of the non-linear response to the absorbed radiant energy as well as the non-linear effect of finite spectral bandwidth. This polynomial is valid only for a given instrument configuration (in terms of operating temperature environment and on-board electronics). It can be described in terms of a gain factor and a **non-linearity**. It is believed that this non-linearity information is valid in orbit. It has been characterised for each of the 24 IR detection

chains and at two operating temperatures. They do not depend on the actual settings of the instrument electronics. All solar channels are linear (within the required accuracy) and therefore their non-linearity is zero. The non-linearity was determined with great precision whereas the gain information was of much lower accuracy.

Currently, the ground based non-linearity and the gain information is used as a **baseline calibration** by IMPF. However, changes of the settings of the on-board electronics need to be taken into account when using the baseline calibration and this is indeed done. Normally, the baseline calibration is corrected using blackbody or vicarious calibration in the Level 1.5 data. During the gap filler period (until 28<sup>th</sup> October 2003), the uncorrected baseline calibration was used for the solar channels where the accuracy requirements are less stringent.

The IMPF uses the non-linearity data from the baseline to correct for the non-linearity in a first processing step (thermal channels only, solar channels are linear). In parallel it uses the gain from the baseline as a first guess for the outgoing radiances. After equalisation, which is based on a statistical analysis of the Earth image and blackbody observations made by the various detectors within a channel, the radiances obtained from all detectors within one channel share the same radiometric scale.

A final adjustment is being made to correct for the fact that the scan **mirror reflectivity varies with scan angle** (or scan position). Therefore, the total gain of the SEVIRI is slightly different for each scan line. For the thermal IR channels, this can be modelled by a linear function of the scan line. The necessary input data are derived from blackbody calibrations performed at different scan positions and is significant only for wavelengths above 6 $\mu$ m. For the solar channels, this data is not available although it is assumed that the scan position dependency is negligible in this spectral range.

### **3.2.2 Blackbody Calibration**

Blackbody calibration and vicarious calibration are treated slightly differently. In the nominal configuration, baseline gain is included with linearisation (also from the baseline) and equalisation (from image statistics) to calculate radiances from raw counts. The blackbody measurements are now used to accurately correct these radiances. Only after this correction, are the radiances (float values) scaled to Level 1.5 pixels using a fixed linear scaling law. This ensures a linear relationship between radiance and Level 1.5 counts (integer values). The scaling law is described by two parameters that are normally kept constant (**baseline scaling**). They are referred to as **cal\_slope** and **cal\_offset** in the **Level 1.5 header**.

For fast implementation the mapping from raw counts to 1.5 counts is performed with the help of a look-up table (LUT). During the image acquisition, the LUT is updated as necessary according to the scan mirror position to account for the variation in the reflectivity in the mirror.

The user must note that **cal\_slope** and **cal\_offset** are fixed scaling factors that will normally not change. They are not related to the calibration process performed to correct the image radiometrically. The result of the blackbody calibration correction applied by the IMPF to the baseline calibration and equalisation is to ensure that the scaling is held constant.

### 3.2.3 Vicarious Calibration

Vicarious calibration coefficients are derived from a comparison of the Level 1.5 image with other sources of information on the outgoing radiance of the earth/atmosphere. This can be radiative transfer calculations over targets of known properties or data from other satellites or both. Currently the MPEF creates vicarious calibration coefficients for the thermal channels using a radiative transfer model over clear ocean targets. The vicarious calibration of the solar channel relies on the SEVIRI Solar Channel Calibration (SSCC) algorithm, which is based upon radiative transfer simulation over bright desert and sea targets accounting for the spectral response of the calibrated channels. The vicarious calibration is averaged over a long period, about 5 day, relying on the IMPF maintaining the calibration sensibly constant over such periods.

All vicarious calibration information is based on Level 1.5 images that are calibrated by the IMPF in any case. When the use of vicarious calibration is enabled in the IMPF, the content of the IMPF Level 1.5 image pixels remains unchanged. It is the annotation that is corrected. In this case, the numerical values of **cal\_slope** and **cal\_offset** in the **Level 1.5 header** are changed according to the vicarious calibration.

#### 3.2.3.1 Vicarious Calibration in the Thermal Channels

Even when the use of vicarious calibration is enabled in the IMPF, the blackbody data is still used to populate the Level 1.5 image pixels. The Level 1.5 image pixels are populated using the baseline gain, baseline non-linearity, the equalisation and the blackbody data. The baseline scaling law is used to go from float radiance to integer Level 1.5 image pixels. Then, the **annotation in the header (cal\_slope and cal\_offset)** is replaced by values obtained from the vicarious calibration based on Level 1.5 image data.

#### 3.2.3.2 Vicarious Calibration in the Solar Channels

In the solar channels there is no blackbody calibration. Therefore, the Level 1.5 image pixels are populated using the baseline gain (solar channels are linear) and the equalisation. The baseline scaling law is used to go from float radiance to integer Level 1.5 image pixels. Then, the **annotation in the header (cal\_slope and cal\_offset)** is replaced by values obtained from the vicarious calibration based on Level 1.5 image data.

## 3.3 Current Operational Baseline

### 3.3.1 Thermal Channels

The thermal channels are calibrated using the **on-board blackbody calibration** (more precisely: using method 3, see section 4, below). The **baseline non-linearity** is used to correct for the non-linear behaviour of the detectors. The scaling is chosen so that the available dynamic range in the Level 1.5 pixels is fully used but no saturation in the Level 1.5 images occurs. Hence, **cal\_slope and cal\_offset are kept constant**. Vicarious calibration is not used for calibration but the information is available and used for monitoring and quality control.

### 3.3.2 Solar Channels

The solar channels are calibrated using **vicarious calibration**. The baseline gain is used to populate the Level 1.5 images but the baseline scaling is adjusted so that the **Level 1.5 pixel counts are very close to the raw counts**. In the Level 1.5 header, **cal\_slope and cal\_offset are updated by the MPEF as soon as a new vicarious calibration is available**.

### 3.3.3 Summary of Level 1.5 Data Production

Level 1.5 MSG data as produced by EUMETSAT contain rectified SEVIRI images in a 10 bit digital format. The images are not only geolocated and transformed to a GEOS projection, they are also representing a fixed radiometric scale. This scale is provided to the user via two linear scaling parameters in the image header (**cal\_slope** and **cal\_offset**). In the case of the solar channels they refer to the vicarious calibration and in the case of the thermal channels they state a pure scaling law for the radiances obtained from the blackbody calibration. From here, the user can reproduce the radiance for each spectral band by the relation:

$$L = cal\_offset + (cal\_slope \times Level\ 1.5\ Pixel\ Count) \text{ (expressed in } mWm^{-2}sr^{-1}(cm^{-1})^{-1} \text{)}$$

The radiometric processing from Level 1.0 (raw data) to Level 1.5 is performed in the following steps:

For the thermal channels:

1. **Linearisation:** The non-linearity of the detection chains has been established on ground. This information is used to remove the effects of non-linearity from the measurement.
2. **Conversion into radiances.** A baseline conversion is performed to go from counts into radiances. Changes of the detection chain settings on-board are corrected for.
3. **Equalisation:** Remaining inequalities between detectors of a given channel are corrected for using raw image statistics.
4. **Blackbody Calibration:** The calibration allows correcting the preliminary estimate of the radiance into accurate numbers.
5. **Scaling.** To store the radiance values in the foreseen 10-bit integer format, a linear scaling is performed using "cal\_slope" and "cal\_offset". These are chosen so that the necessary dynamic range falls into the available interval [0, 1023]. When converting raw data into Level 1.5 image pixels, also the correction for the scan angle dependency of the gain is taken into account. Thus, "cal\_slope" and "cal\_offset" provide the correct scaling for the full Level 1.5 images.

For the solar channels:

1. **Conversion into radiances.** In fact solar channels are linear. A baseline conversion is performed to go from counts into radiances.
2. **Equalisation:** Remaining inequalities between detectors of a given channel are corrected for using raw image statistics.
3. **Scaling:** To store the radiance values in the foreseen 10 bit integer format, a scaling is performed that in practise creates Level 1.5 pixels which are very close to the raw count value.

4. Vicarious calibration: cal\_slope and cal\_offset are determined by vicarious calibration and put into the Level 1.5 Header. An update is only when a new vicarious calibration becomes available.

The consequence of this approach is illustrated in Figure 1.

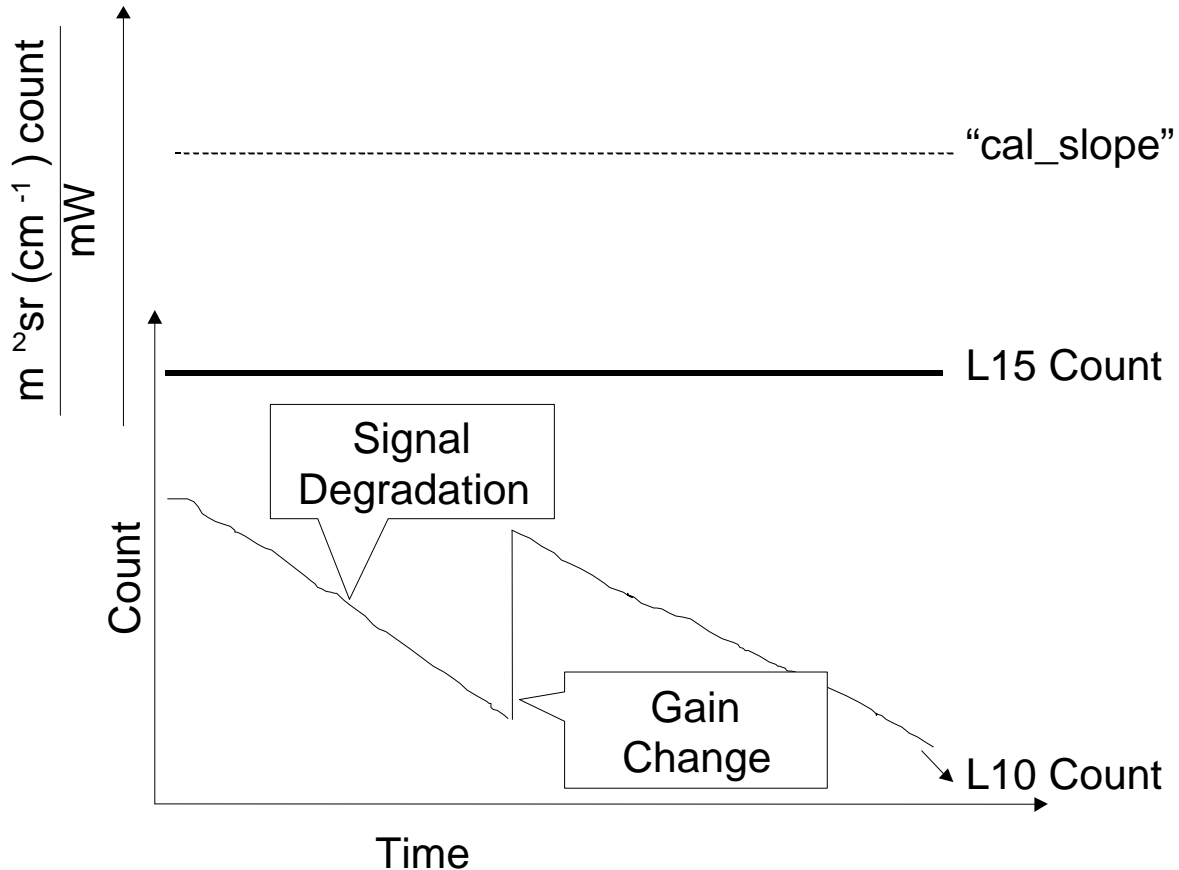


**Figure 1 – Schematic of the Scaling of Level 1.5 Counts**

Figure 1 shows the Level 1.0 count and the Level 1.5 count of an idealised stable IR target. The raw Level 1.0 count degrades in time as contamination increases. At some point, a gain change is performed to maintain image quality. During all this time, the Level 1.5 count remains stable as the instrument calibration is used to remove degradation effects from the Level 1.5 image. Also, a gain change is transparent to the user. "cal\_slope" represents a pure scaling constant for target radiances to Level 1.5 pixel counts, which is not affected by instrument degradation or gain changes.

## **4 DETAILS ON BLACKBODY CALIBRATION**

### **4.1 The SEVIRI Telescope**

In the SEVIRI three mirror telescope, the incoming Earth radiance is reflected on the primary telescope mirror M1 by a flat scan mirror that is used to adjust the line of sight in the North-South direction for scanning. The primary mirror transfers the light through the central hole of the scan mirror onto the secondary and tertiary mirrors, M2 and M3, from where the light is focussed onto the detectors via a relay optic. A black baffle in the centre of the M1 mirror reduces the stray light that enters the telescope. The large size of the entrance aperture makes it impossible to put a calibration source there. However, a small black body source can be placed near the field stop in the intermediate focal plane between primary and secondary mirror. The "front optics" (scan mirror, mirror M1, M1 baffle) cannot be seen from the detector when the blackbody source is in place, whereas the "back optics" (M2, M3 and following relay optics) are behind the blackbody calibration source so are seen.

During each satellite rotation, deep space measurements are taken corresponding to zero input radiance. The irradiance at detector level now corresponds to the self-radiation of the instrument only.

The signal of the deep space measurements is subtracted on-board automatically from the Earth measurements after digitisation to cancel the contribution of the front optics and any other internal offset from the useful signal. (This is performed on-board with 12 bit precision to reduce quantisation errors.) When the blackbody is in place, the deep space measurements from the image line prior to the blackbody measurement are subtracted. The signal received at the detector during black body observation does not contain any information from the front optics (because the blackbody physically covers it). However, the subtraction process introduces again information from the front optics obtained during the deep space measurements into the digital counts sent to Earth (Figure 2). With SEVIRI, the effect of the front optics on the Earth measurement and the black body measurement needs to be considered in a calibration model. A standard blackbody-space (two-point) calibration method is not appropriate for SEVIRI.

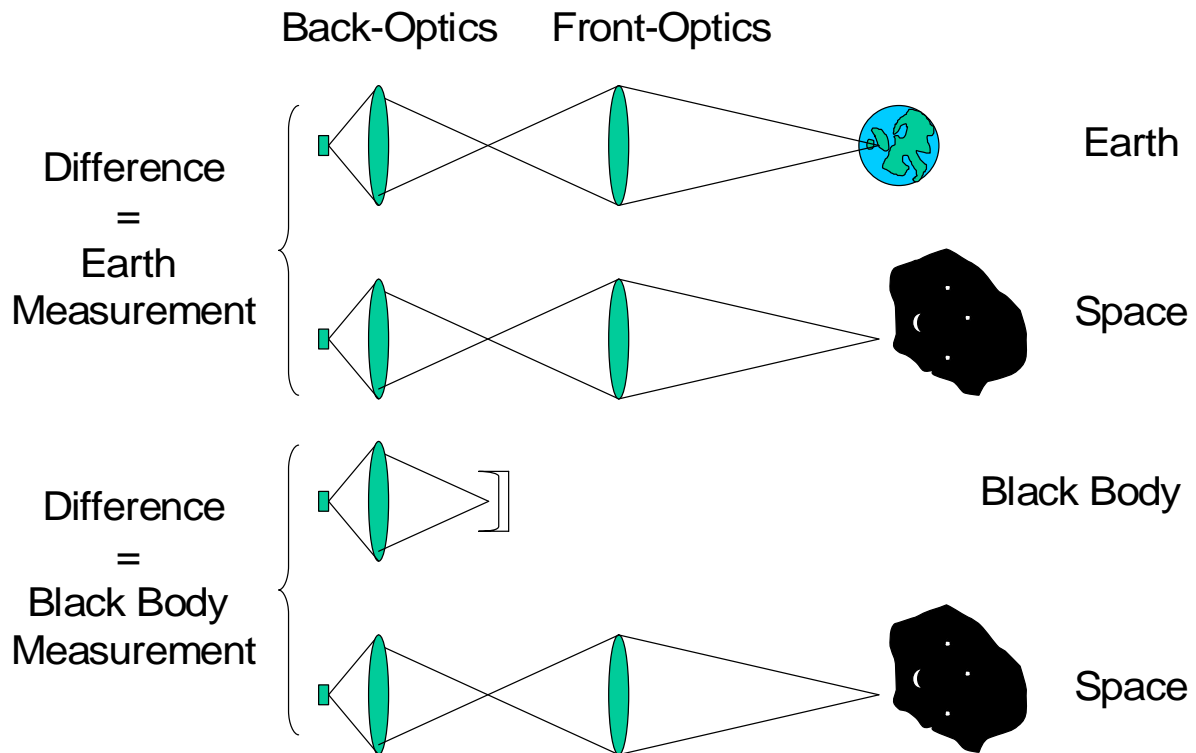


Figure 2 – Measurements and Direct Offset Correction

#### 4.2 Black Body Calibration

The signal irradiance as received at the detector level is the product of three factors:

1. The target radiance, either from Earth or black body
2. The total optical loss accrued during passage through the instrument
3. The solid angle under which the detector collects the radiation. The opening cone for the incoming radiation is determined by the diameter and the focal length of the optical system

The calibration is performed in two steps: at ambient temperature plus a measurement with the blackbody heated to about 20K above ambient. This pair allows for the calibration of the "back optics" in a two-point calibration. Knowing the gain of the back optics, the estimation of the gain of the complete system needs some assumptions and simplifications such as assuming a common temperature of the front optics etc. There are currently three models available to perform an interpretation of the blackbody measurement. They are referred to as "blackbody models". Details on the blackbody models will be discussed later.

All three models have in common that they use the **baseline calibration in the IMPF** as a first step. They also use the **equalisation** data to remove remaining differences between detectors of a given channel. Level 1.0 instrument counts from each detector acquired during a blackbody measurement would therefore be converted into raw radiance estimate,  $R$ . This raw radiance estimate,  $R$ , is the same for all detectors in a chain (because of the equalisation) and has a (still yet unknown) linear relationship to the true radiance (because of the linearisation contained in the baseline calibration). The values are averaged over all blackbody samples and all detectors so that there is a **single value of  $R$  for each IR channel**.

This value is then used as input to the blackbody models. As the input to the blackbody model is already a radiance estimate, the **gain calculated will be in units of radiance per radiance and therefore unitless**. This gain " $G_{total}$ " (not to be confused with  $G_{TOT}$  as discussed in section 5) can therefore be interpreted as a pure correction to the baseline calibration. In case the baseline calibration is correct,  $G_{total}=1$ .

$G_{total}$  is reported for each blackbody model in the header. As the gain depends on the scan position during the measurement (which is modelled as a linear function of scan line), the number reported in the Level 1.5 header is corrected for and refers to fixed datum position, normally the nominal scan position for a blackbody line.

### 4.3 Blackbody Models

A measurement at ambient temperature plus a measurement with the blackbody heated to about 20K above ambient is used for the calibration. The calibration of the "back optics" is performed in a two-point measurement taking into account the viewing geometry and potential changes of the thermal environment in the time between the calibrations. The self-radiation of the front optics and the attenuation of it need to be modelled. There are three models available.

#### 4.3.1 Model 1 (EUMETSAT Scheme)

The EUMETSAT scheme assumes that the measurement contains contributions from the blackbody (that are known) and from the front optics (introduced by the space view and that are unknown). This is the simplest possible scheme and so provides a baseline. However, a pair of two measurements allows for solving for the gain of the back optics  $G_{back}$  and the radiance contributions from the front optics, assuming that the temperature of the front optics does not change significantly between the two measurements. The full gain can then be calculated as:

$$G_{total} = G_{back} \tau_{M1} \tau_{scan}$$

where  $\tau_{M1}$  and  $\tau_{scan}$  are the transmittances of the mirror M1 and the scan mirror, respectively. These need to be provided from ground testing. Because the value of  $\tau_{scan}$  depends on the scan angle, the result  $G_{total}$  of Method 1 refers always to the scan line of which  $\tau_{scan}$  is given for.

#### 4.3.2 Model 2 ("Portsmouth Scheme", "MMS-P Scheme")

The MMS-P scheme uses the same general approach as the EUMETSAT scheme. However, the determination of the front optics self-radiance is difficult and may suffer from observational errors (as hot and cold blackbody observations are very often close together compared to the full dynamic range). Calibration can be performed over the full dynamic range, only if the self-radiation is precisely known. There can be a bias in the evaluation of the self-radiation if the ground characterised parameters drift. Any such drift will be small so we can approximate the true contribution from the front optics by the estimated self-radiation and a new parameter  $g_f$  where  $g_f$  is close to 1 and very slowly varying.  $g_f$  can be averaged over many observations, the current average  $g_f$  being updated by:

$$g_f(n+1) = (1 - \beta_g)g_f(n) + \beta_g g_f(n)$$

where  $\beta_g$  is a pre-defined averaging constant. This approach should be more stable than the EUMETSAT scheme. Also, once  $g_f$  is determined by a hot/ambient blackbody measurement pair, it is possible to obtain an update to the gain by just using a single ambient temperature blackbody measurement under the assumption that the properties of the front optics haven't changed.

#### **4.3.3 Model 3 ("Toulouse Scheme", "MMS-F Scheme")**

Knowing the gain of the back optics, the self-radiation of the front optics can be measured when viewing cold space (= zero input). In fact, this needs only a single measurement with the blackbody at ambient because the space count is always subtracted. The assumption that the reflectance of the mirrors plus their emissivity equals 1 when integrated over the field of view, allows estimating the front optics transmittance from its temperature and its self-radiation. To this end, it is assumed that all elements of the front optic have the same temperature. The temperature of the front optic is derived as a weighted mean of the various temperature sensors in the area. The elements of the front optics then can be treated as Planck radiators of a given emissivity. It turns out that the blackbody measurement then can be described in terms of the Planck radiance of the blackbody and the front optics as well as the back optics gain  $G_{\text{back}}$  and the front optics transmission  $\tau_{M1}\tau_{\text{scan}}$ . With the back optics responsivity and the front optics transmittance the full instrument gain can be calculated. Again, because the value of  $\tau_{\text{scan}}$  depends on the scan angle, the result  $G_{\text{total}}$  of Method 2 refers always to the scan line of which  $\tau_{\text{scan}}$  is given for.

#### **4.4 Application of Blackbody Calibrations in the Thermal channels**

$G_{\text{total}}$  is always calculated by all methods and average values for all three methods are maintained. Only one value is selected by warm start and used for calibration, the selection being user configurable.

The  $G_{\text{total}}$  from the selected method is used to calculate a calibration constant for each thermal channel simply by  $K_{\text{cal}}=1/G_{\text{total}}$ . It is also possible to configure  $K_{\text{cal}}=1$ .  **$K_{\text{cal}}$  is reported in the header as well as all the values for  $G_{\text{total}}$  of each method.**

Since the reflectivity of the scan mirror depends on the scan angle, the value for  $G_{\text{total}}$  always refers to specific scan position. The values reported in the header refer to a fixed scanning mirror reference. This fixed position is configured to be the nominal scan position during a blackbody calibration. When creating the Level 1.5 image, the variation of the scan mirror reflectivity during the image acquisition is accounted for.

## 5 INSTRUMENT GAIN CHANGES AND REDUCED GAIN FOR PERFORMANCE ASSESSMENT

The total gain  $G_{TOT}$  (not to be confused with the correction  $G_{total}$  derived from the blackbody, see section 4) is defined as follows:

$$G_{TOT} = \left. \frac{\partial(\text{raw count})}{\partial L_{\lambda}} \right|_{L_{\lambda} = 0}$$

This describes the relationship between incoming radiance and raw instrument count. The gain depends on the detection chain settings. There are various steps of electronic amplification. Firstly, an adjustable pre-amplifier unit (PU) amplifies the detector current or voltage. The output is further amplified at the Main Detection Unit (MDU) that contains also the ADC. The final amplification and digitisation can be described in terms of 4 parameters  $n_G$ ,  $n$ ,  $p$  and  $q$ . Therefore, in order to investigate the responsivity independently from the gain settings, the gain  $G_{TOT}$  of each chain has been split into a fixed part  $G_0$  and a variable part that depends on the electronics setting. ( $G_{TOT} = G_0 * G_{3PU}(n_G) * 1.2^{n-3} * (1+p/2048) * 2^q$   $n_G$ ,  $n$ ,  $p$  and  $q$  are telemetry values for the detection chain settings for the PU gain, MDU coarse, fine and output gains, respectively.) The fixed part of the gain,  $G_0$ , therefore does not show any gain changes but all instrument degradations (Figure 1). Neither the gain  $G_{TOT}$  nor the reduced gain  $G_0$  is easily available from the Level 1.5 header or trailer. They are, however, used to monitor the state of the instrument at EUMETSAT. For presentation purposes, the  $G_0$  of all chains are normalised in the figures of this paper.

### 5.1 Degradation and Decontamination

Calibration measurements are performed at regular intervals using the on-board blackbody (Figure 3). The detection chains show a nearly linear trend in time towards lower response. The speed of degradation tends to increase with wavelength.

The degradation is mainly due to collection of contaminants at the cold part of the optics. This can be removed by a short heating period for the cold optics to evaporate the contaminants. Figure 4 clearly shows the degradation and the decontamination events. A first decontamination was performed shortly after launch before the start of the imaging mission. The second decontamination was performed between 18 March (SEVIRI into Standby) and 24 March 2003 (first images after decontamination). After decontamination, the gains and offsets had to be re-adjusted. Decontamination itself was performed without imaging, as it took place during eclipse (to save power). Detection chain radiometric response increased between 10% and 140% after decontamination. A third decontamination was performed between 11 and 14 August 2003. This time, SEVIRI was imaging on the HRV, VIS and NIR channels. After resuming imaging with the IR channels, new adjustments to the detection chains were necessary.

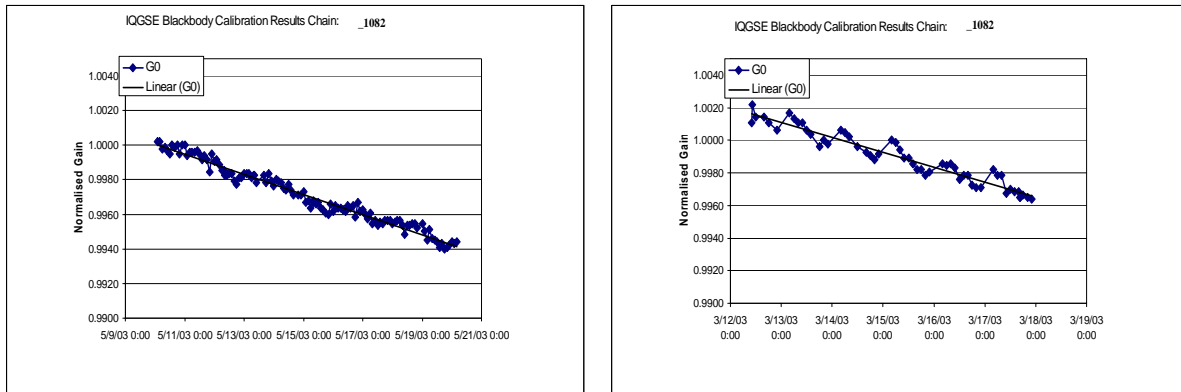


**Figure 3 – Calibration Results for the IR 10.8 Channel outside an Eclipse Season (left) and during an Eclipse Season (right)**

Prior to the August decontamination, SEVIRI IR channels were operated at 85K (not shown) rather than 95K. After decontamination, 95K was used again. However, this made a comparison of the response between before and after the August decontamination impossible. Therefore, a comparison was made between the responses prior the decontamination in March and after the decontamination in August. The detection chain radiometric response increased between 10% and 150% after the August decontamination with respect to March. This seems to indicate that the radiometer is now in an even better state than after the March decontamination. This was expected because the August decontamination was initiated from a much lower level of contamination than in March (see Figure 4). Hence, the decontaminations allowed to recover instrument gains close to the gains measured at instruments and S/C levels during the ground tests.

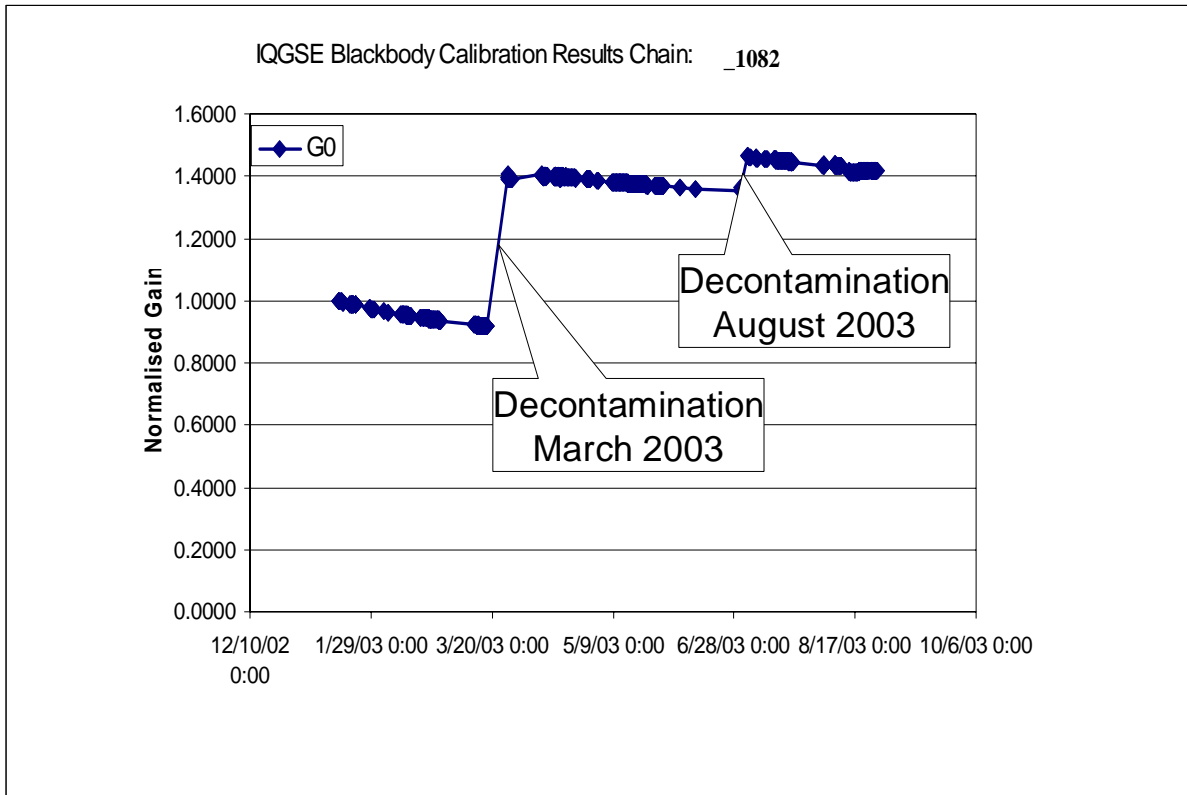


**Figure 4 – Calibration Results for the IR 10.8 channel during 2003**

## 5.2 Eclipse Season

During an eclipse season, the Earth is between the Sun and the spacecraft every night for up to 1½ hours. Among other things, the temperature of the optics of SEVIRI drops significantly. The detector temperatures, however, are stabilised and don't change. Figure 3 compares calibration results obtained inside and outside an eclipse season. The variations in the calibration results are much higher during an eclipse season than outside. It is believed that this is caused by the strong temperature change. However, the performance is still excellent.

## **6 REFERENCE DOCUMENTS**

1. MSG Level 1.5 Image Product Oversight Panel - Meeting 2, EUM/OPS-MSG/MIN/06/0361, v1, 28 August 2006 and Delta 18. September 2006.
2. MSG END-User Requirements Document EUM/MSG/SPE/013.
3. Vermote, E. F., D. Tanre, J. L. Deuze, M. Herman, and J. J. Morcrette (1997) Second simulation of the satellite signal in the solar spectrum, 6S: An overview. IEEE Transactions on Geoscience and Remote Sensing 35, 675–686.
4. Govaerts, Y.M., Arriaga, A., and Schmetz, J. (2001) Operational vicarious calibration of the MSG/SEVIRI solar channels, Advances in Space Research, 28, 21-30.

## APPENDIX A IMPLEMENTATION OF THE BLACKBODY MODELS (FROM VOLUME Q OF THE IMPF DDD)

The following symbols are used to denote the various optical components and instrument characteristics of the SEVIRI instrument.

### Optical Components

BB	Blackbody Calibration Source
scan	Scan Mirror
M1	M1 Primary Mirror
M1baf	Primary Mirror Baffle
M2	M2 Secondary Mirror
M3	M3 Tertiary Mirror
IRO	Infra Red Relay Optics

### Instrument Characteristics

$G_{elec}$ (= $G_{MDU-out}G_{MDU-f}G_{MDU-O}G_{MDU-C}G_{PU}$ )	gain of detector electronics
$R_d$	integrated response of detector over channel
$\epsilon_{BB}, \epsilon_{scan}, \epsilon_{M1}, \epsilon_{M1baf}$	emissivity of optical components
$\rho_{BB}, \rho_{scan}, \rho_{M1}, \rho_{M1baf}$	spectral diffusion coefficients of optical components
$\tau_{scan}, \tau_{M1}, \tau_{M2}, \tau_{M3}$	reflectances of mirrors
$\tau_{IRO}$	transmittance of IR optics
A	effective area of detector
$U_{proj}$	effective angular aperture of telescope
$U_{proj}v^2/(1-\xi^2)$	effective angular aperture of central obscuration, defined by aperture stop
v	field stop ratio
$\xi$	linear central obscuration ratio

Variables used in BB Processing

$T_{cal}, T_{M1baf}, T_{M1}, T_{scan}$	Temperatures of optical components
$L(T)$	Radiation density of a black body at temperature T
$\mathcal{H} = \tau_{IRO} \times$ Electronics transfer function	Radiometric processing transfer function.
R	Requantised output
R'	Radiation incident on telescope
$R_{back}$	Signal from back optics radiation and electronic noise.

For convenience we define the following derived quantities

$G_{back} = \mathcal{H} G_{elec} U_{proj} A R_d \tau_{M2} \tau_{M3}$ $= (\mathcal{H} G_{elec} U_{proj} A R_d \tau_{M2} \tau_{M3})_{nom} / K_{cal}$	Instrument and processing gain as seen by Blackbody
$G_{total} = G_{back} \tau_{M1} \tau_{scan}$	Overall SEVIRI instrument gain
$\phi = v^2 / [(1 - \xi^2) \tau_{M2} \tau_{M3}]$	Ratio of the 'direct view' aperture to the total effective aperture

The detector and electronics characteristics are non-linear and dependent on various externally controlled parameters. We treat the output of the instrument for which we require calibration to be R, the value obtained after applying the radiometric correction LUT. Here the LUT is that specifically defined for calibration that does not contain the calibration factor,  $K_{cal}$ , the unknown we wish to find from black body processing, nor the output scaling.

The following equations can be derived for the system output when looking at the Earth, dark space and the calibration target. For derivations see RD 4, EUMETSAT technical note 'The On-Board Calibration Model for MSG'.

Earth Looking

$$R_{scn} = G_{back} \tau_{M1} \tau_{scan} R'_{scene} = G_{total} R'_{scene}$$

All input except that from the incident light on the front optics is removed by the DCR subtraction.

Dark Space

$$R_{DCR} = R_{back} + G_{back} [(\epsilon_{M1} + \rho_{M1})L(T_{M1}) + \phi(\epsilon_{M1baf} + \rho_{M1baf})L(T_{M1baf}) + \tau_{M1}(\epsilon_{scan} + \rho_{scan})L(T_{scan})]$$

$R_{back}$  is the self-radiation of the back optics, the remaining terms being the self-radiation and diffused scattering of the M1 mirror, M1 baffle and the scan mirror. Here it is assumed that

the temperature of the surroundings of each component equals the temperature of the component.

Calibration

$$R_{cal}(T_{cal}) = R_{back} + G_{back}(1 + \phi)\epsilon_{BB}L(T_{cal}) + G_{back}(1 + \phi)\rho_{BB}L(T_{cal}^*) - R_{DCR}$$

The term  $G_{back}(1 + \phi)\rho_{BB}L(T_{cal}^*)$  represents radiation from the BB surroundings scattered off the BB.

Substituting for  $R_{DCR}$  gives

$$R_{cal}(T_{cal}) = G_{back}(1 + \phi)\epsilon_{BB}L(T_{cal}) - G_{back}[(\epsilon_{M1} + \rho_{M1})L(T_{M1}) + \phi(\epsilon_{M1baf} + \rho_{M1baf})L(T_{M1baf}) + \tau_{M1}(\epsilon_{scan} + \rho_{scan})L(T_{scan}) - (1 + \phi)\rho_{BB}L(T_{cal}^*)]$$

Define the quantity

$$f(T_{scan}, T_{M1}, T_{M1baf}, T_{cal}^*) = [(\epsilon_{M1} + \rho_{M1})L(T_{M1}) + \phi(\epsilon_{M1baf} + \rho_{M1baf})L(T_{M1baf}) + \tau_{M1}(\epsilon_{scan} + \rho_{scan})L(T_{scan}) - (1 + \phi)\rho_{BB}L(T_{cal}^*)]$$

Then

$$R_{cal}(T_{cal}) = G_{back}(1 + \phi)\epsilon_{BB}L(T_{cal}) - G_{back} f(T_{scan}, T_{M1}, T_{M1baf}, T_{cal}^*)$$

Here we have made the assumptions that the temperature of the surroundings of a mirror are the same as a mirror, e.g.  $T_{M1} = T_{M1}^*$ . It is not clear what value should be used for  $T_{cal}^*$ , the implementation has  $T_{cal}^* = T_{cal}$ . Fortunately the contribution is small since  $\rho_{BB} \sim 0$ .

To obtain a calibration we require to find  $G_{back}\tau_{M1}\tau_{scan}$ , the relation between the incident radiation and the radiation measure at the system output. The two baseline methods use values of  $\tau_{M1}$  and  $\tau_{scan}$  obtained from ground characterisation so calibration reduces to finding  $G_{back}$ .

### A.1 Method 1 (EUMETSAT Scheme)

An estimate of  $G_{back}$  is obtained from a hot and cold black body observation pair.

$$R_{cal}(T_{cold}) = G_{back}(1 + \phi)\epsilon_{BB}L(T_{cold}) - G_{back} f_1(T_{scan}, T_{M1}, T_{M1baf}, T_{cal}^*)$$

$$R_{cal}(T_{hot}) = G_{back}(1 + \phi)\epsilon_{BB}L(T_{hot}) - G_{back} f_2(T_{scan}, T_{M1}, T_{M1baf}, T_{cal}^*)$$

Where  $T_{cal} = T_{cold}$  and  $f = f_1$  for the cold BB observation and  $T_{cal} = T_{hot}$  and  $f = f_2$  for the hot BB observation. Then

$$R_{cal}(T_{hot}) - R_{cal}(T_{cold}) = G_{back}[(1 + \phi)\epsilon_{BB}(L(T_{hot}) - L(T_{cold})) + f_1(T_{scan}, T_{M1}, T_{M1baf}, T_{cal}^*) - f_2(T_{scan}, T_{M1}, T_{M1baf}, T_{cal}^*)]$$

$$G_{back} = (R_{cal}(T_{hot}) - R_{cal}(T_{cold}))[(1 + \phi)\epsilon_{BB}(L(T_{hot}) - L(T_{cold})) + f_1(T_{scan}, T_{M1}, T_{M1baf}, T_{cal}^*) - f_2(T_{scan}, T_{M1}, T_{M1baf}, T_{cal}^*)]^{-1}$$

The original EUMETSAT scheme assumes that the front optics temperatures do not change between the hot and cold observations, then  $f_1 = f_2$ . In this case the above equation reduces to

$$G_{back} = (R_{cal}(T_{hot}) - R_{cal}(T_{cold}))[(1 + \phi)\epsilon_{BB}(L(T_{hot}) - L(T_{cold}))]^{-1}$$

The overall system gain is then given by

$$G_{total} = G_{back} \tau_{M1} \tau_{scan}$$

$G_{total}$  can then be averaged over successive measurements by updating the current average  $G_{total}$  by

$$G_{total}(n+1) = (1 - \beta_{cal}) G_{total}(n+1) + \beta_{cal} G_{total}(n)$$

where  $\beta_{cal}$  is a predefined averaging constant.

Since both  $R$  and  $L$  have units of  $Wm^{-2}sr^{-1}\mu m^{-1}$ ,  $G_{total}$  is dimensionless.

## A.2 Method 2 ("Portsmouth Scheme", "MMS-P Scheme")

$G_{back}$  as derived by method 1 can have observational errors. The two points  $L(T_{hot})$  and  $L(T_{cold})$  are close together at one end of the radiance dynamic range. Small observational errors can give large calibration errors at the extreme ends of the dynamic range. If the observation errors are systematic, or  $G_{back}$  varies significantly between hot/cold pair observations then averaging over many observations may not reduce the error. Calibration can be performed over the full dynamic range,  $L(0)$  to  $L(T_{cal})$ , if  $f(\ )$  is precisely known. There can be a bias in the evaluation of  $f(\ )$  if the ground characterised parameters drift. Any drift will be small so we can approximate the true contribution from the front optics represented by  $f(\ )$  by a  $g_f f(\ )$  where  $g_f$  is close to 1 and very slowly varying. Using this in the calibration equations, **12-8** and **12-9**, gives

$$R_{cal}(T_{cold}) = G_{back}(1 + \phi)\epsilon_{BB}L(T_{cold}) - G_{back}g_f f_1(T_{scan}, T_{M1}, T_{M1baf}, T_{cal}^*)$$

$$R_{cal}(T_{hot}) = G_{back}(1 + \phi)\epsilon_{BB}L(T_{hot}) - G_{back}g_f f_2(T_{scan}, T_{M1}, T_{M1baf}, T_{cal}^*)$$

We use a hot/cold BB observation pair to solve for  $g_f$ . Eliminating  $G_{back}$  by dividing the equations gives

$$\begin{aligned} & R_{cal}(T_{cold})[(1 + \phi)\epsilon_{BB}L(T_{hot}) - g_f f_2(T_{scan}, T_{M1}, T_{M1baf}, T_{cal}^*)] \\ &= R_{cal}(T_{hot})[(1 + \phi)\epsilon_{BB}L(T_{cold}) - g_f f_1(T_{scan}, T_{M1}, T_{M1baf}, T_{cal}^*)] \\ (1 + \phi)\epsilon_{BB}[ & R_{cal}(T_{hot})L(T_{cold}) - R_{cal}(T_{cold})L(T_{hot})] \\ &= g_f[R_{cal}(T_{hot})f_1(T_{scan}, T_{M1}, T_{M1baf}, T_{cal}^*) - R_{cal}(T_{cold})f_2(T_{scan}, T_{M1}, T_{M1baf}, T_{cal}^*)] \\ & g_f = (1 + \phi)\epsilon_{BB}[ R_{cal}(T_{hot})L(T_{cold}) - R_{cal}(T_{cold})L(T_{hot})] \\ & \times [R_{cal}(T_{hot})f_1(T_{scan}, T_{M1}, T_{M1baf}, T_{cal}^*) - R_{cal}(T_{cold})f_2(T_{scan}, T_{M1}, T_{M1baf}, T_{cal}^*)]^{-1} \end{aligned}$$

$g_f$  can be averaged over many observations, the current average  $g_f$  being updated by

$$g_f(n+1) = (1 - \beta_g)g_f(n) + \beta_g g_f(n)$$

where  $\beta_g$  is a predefined averaging constant.

$G_{total}$  can now be estimated from any black body observation by substituting  $g_f$  for  $G_{back}$ .

$$R_{cal}(T_{cal}) = G_{back}(1 + \phi)\epsilon_{BB}L(T_{cal}) - G_{back}g_f f(T_{scan}, T_{M1}, T_{M1baf}, T_{cal}^*)$$

$$G_{back} = R_{cal}(T_{cal}) / [(1 + \phi)\epsilon_{BB}L(T_{cal}) - g_f f(T_{scan}, T_{M1}, T_{M1baf}, T_{cal}^*)]$$

$$G_{total} = G_{back}\tau_{M1}\tau_{scan}$$

$G_{total}$  can then be averaged as for method 1.  $G_{total}$  is thus updated every repeat cycle for which there is a valid BB observation, using the appropriate averaging.  $g_f$  is only updated as a result of a hot calibration part of a hot/cold pair.

The ability to derive  $G_{total}$  from a single BB observation using this method means that shorter term variations can be tracked than when using the other methods.

### A.3 Method 3 ("Toulouse Scheme", "MMS-F Scheme")

This third method differs fundamentally in that it gives  $G_{total}$  directly without any need for externally characterised values of  $\tau_{M1}\tau_{scan}$ . However other assumptions have to be made. Most significantly it is assumed that for the M1 mirror and for the Scan mirror

$$\epsilon + \rho + \tau = 1, \quad \epsilon + \rho = 1 - \tau$$

This is certainly true integrated over the full sphere, being conservation of energy. It is not clear how precisely valid this is for the solid angle seen by the telescope.

$$R_{cal}(T_{cal}) = G_{back}(1 + \phi)\epsilon_{BB}L(T_{cal}) - G_{back}[(1 - \tau_{M1})L(T_{M1}) + \phi(1 - \tau_{M1baf})L(T_{M1baf}) + \tau_{M1}(1 - \tau_{scan})L(T_{scan}) - (1 + \phi)\rho_{BB}L(T_{cal}^*)]$$

It is further assumed that the black body target and the M1 baffle are perfect Black Bodies so that  $\epsilon = 1$  and  $\tau = 0$ . Then

$$R_{cal}(T_{cal}) = G_{back}(1 + \phi)L(T_{cal}) - G_{back}[(1 - \tau_{M1})L(T_{M1}) + \phi L(T_{M1baf}) + \tau_{M1}(1 - \tau_{scan})L(T_{scan})]$$

$$R_{cal}(T_{cal}) = G_{back}[(1 + \phi)L(T_{cal}) - L(T_{M1}) - \phi L(T_{M1baf})] + G_{back}[\tau_{M1}L(T_{M1}) - \tau_{M1}L(T_{scan})] + G_{back}\tau_{M1}\tau_{scan}L(T_{scan})]$$

If  $T_{M1} = T_{scan}$  then the second term is zero. Further if  $T_{M1} = T_{M1baf}$  then this is an equation in just two unknowns,  $G_{back}(1 + \phi)$  and  $G_{back}\tau_{M1}\tau_{scan} = G_{total}$ .

$$R_{cal}(T_{cal}) = G_{back}(1 + \phi)[L(T_{cal}) - L(T_{M1})] + G_{total}L(T_{scan})$$

MMS-F make the further approximation that  $T_{M1} = T_{scan} = T_{front}$ , an equivalent front optics temperature. It is not essential to assume that  $T_{scan}$  is the same as that of the rest of the front optics for this method to work. However once the temperature uniformity of the rest of the front optics is assumed this last assumption is minor and greatly simplifies the method. It is shown that the errors made by assuming temperature uniformity are of the order of 0.1 K. They are minimised if the effective front optics temperature is set to

$$T_{front} = \frac{\varepsilon_{M1}(1-\xi^2)T_{M1} + \varepsilon_{scan}\tau_{M1}(1-\xi^2)T_{scan} + \frac{v^2}{\tau_{M2}\tau_{M3}}T_{M1baf}}{\varepsilon_{M1}(1-\xi^2) + \varepsilon_{scan}\tau_{M1}(1-\xi^2) + \frac{v^2}{\tau_{M2}\tau_{M3}}}$$

The parameters used in evaluating this expression are the ground characterised values. Errors in these contribute to an already small quantity so have minimal effect.

For the cold and hot calibration observations this then gives

$$R_{cal}(T_{cold}) = G_{back}(1 + \phi)[L(T_{cold}) - L(T_{front})] + G_{total}L(T_{front})$$

$$R_{cal}(T_{hot}) = G_{back}(1 + \phi)[L(T_{hot}) - L(T'_{front})] + G_{total}L(T'_{front}).$$

These can be solved for  $G_{back}(1 + \phi)$  and  $G_{total}$ .

$$G_{total} = \{R_{cal}(T_{cold})[L(T_{hot}) - L(T'_{front})] - R_{cal}(T_{hot})[L(T_{cold}) - L(T_{front})]\}$$

---


$$\{L(T_{hot})L(T_{front}) - L(T_{cold})L(T'_{front})\}$$

$$G_{back}(1 + \phi) = \{R_{cal}(T_{hot})L(T_{front}) - R_{cal}(T_{cold})L(T'_{front})\}$$

---


$$\{L(T_{hot})L(T_{front}) - L(T_{cold})L(T'_{front})\}$$

The ratio  $\Delta_f = G_{total} / G_{back}$  is also calculated and gives a measure of  $\tau_{M1}\tau_{scan}$ .  $\tau_{M1}\tau_{scan}$  should be very stable so this value can be averaged over a large number of observations:

$$\Delta_f(n+1) = (1 - \beta_g)\Delta_f(n) + \beta_g\Delta_f(n)$$

$\Delta_f$  can only be updated using a cold/hot pair of blackbody observations. However, for any hot or cold blackbody observations,  $G_{total}$  is obtained using the averaged  $\Delta_f$ :

$$G_{total} = R_{cal}(T_{cal}) / \{ [(1 + \phi) / \Delta_f(n)] [L(T_{cal}) - L(T_{front})] - L(T_{front}) \}$$

#### A.4 Derivation of Calibration Constant $K_{cal}$

$G_{total}$  is always calculated by all methods and average values for all three methods are maintained. Due to scan line dependency of the scan mirror reflectance, the blackbody calibration result  $G_{total}$  always refers to a specific scan line. For methods 1 and 2 the scan mirror reflectance is input as the input value of  $\tau_{scan}$ .  $G_{total}$  derived for method 3 is adjusted to the same reference scan line as  $\tau_{scan}$ . Only one method is selected by warm start and used for calibration, the selection being user configurable.

Internally, IMPF uses the inverse of  $G_{total}$ :  $K_{cal} = 1 / G_{total}$ . The value of  $K_{cal}$  used to scale the image pixels is adjusted line by line to allow for the scan position dependence.